

## Fiber-type differences in muscle mitochondrial profiles

S. C. Leary,<sup>1</sup> C. N. Lyons,<sup>1</sup> A. G. Rosenberger,<sup>2</sup>  
J. S. Ballantyne,<sup>2</sup> J. Stillman,<sup>3</sup> and C. D. Moyes<sup>1</sup>

<sup>1</sup>Department of Biology, Queen's University, Kingston, Ontario K7L 3N6;

<sup>2</sup>Department of Zoology, University of Guelph, Guelph, Ontario, Canada N1G 2W1;

and <sup>3</sup>Hopkins Marine Station, Stanford University, Pacific Grove, California 93950-3094

Submitted 30 January 2003; accepted in final form 3 June 2003

**Leary, S. C., C. N. Lyons, A. G. Rosenberger, J. S. Ballantyne, J. Stillman, and C. D. Moyes.** Fiber-type differences in muscle mitochondrial profiles. *Am J Physiol Regul Integr Comp Physiol* 285: R817–R826, 2003; 10.1152/ajpregu.00058.2003.—Although striated muscles differ in mitochondrial content, the extent of fiber-type specific mitochondrial specializations is not well known. To address this issue, we compared mitochondrial structural and functional properties in red muscle (RM), white muscle (WM), and cardiac muscle of rainbow trout. Overall preservation of the basic relationships between oxidative phosphorylation complexes among fiber types was confirmed by kinetic analyses, immunoblotting of native holoproteins, and spectroscopic measurements of cytochrome content. Fiber-type differences in mitochondrial properties were apparent when parameters were expressed per milligram mitochondrial protein. However, the differences diminished when expressed relative to cytochrome oxidase (COX), possibly a more meaningful denominator than mitochondrial protein. Expressed relative to COX, there were no differences in oxidative phosphorylation enzyme activities, pyruvate-based respiratory rates, H<sub>2</sub>O<sub>2</sub> production, or state 4 proton leak respiration. These data suggest most mitochondrial qualitative properties are conserved across fiber types. However, there remained modest differences (~50%) in stoichiometries of selected enzymes of the Krebs cycle,  $\beta$ -oxidation, and antioxidant enzymes. There were clear differences in membrane fluidity (RM > cardiac, WM) and proton conductance (H<sup>+</sup>/min/mV/U COX: WM > RM > cardiac). The pronounced differences in mitochondrial content between fiber types could be attributed to a combination of differences in myonuclear domain and modest effects on the expression of nuclear- and mitochondrially encoded respiratory genes. Collectively, these studies suggest constitutive pathways that transcend fiber types are primarily responsible for determining most quantitative and qualitative properties of mitochondria.

skeletal muscle; oxidative phosphorylation; reactive oxygen species; membrane fluidity; proton leak; energy metabolism

---

STRIATED MUSCLES GENERALLY rely on mitochondrial metabolism for energy production but there are many differences in mitochondrial qualitative and quantitative properties among muscles. Mitochondrial abundance can be vastly different among fiber types, physiological state, environmental conditions, and species. For instance, mitochondrial volume in vertebrate stri-

ated muscles can range from <1% of cell volume to >45% of cell volume (see Refs. 30, 40). Muscle mitochondrial content is a reflection of the relative importance of mitochondria to the energy budget of each fiber type. Although these dramatic differences in mitochondrial quantity are well established, muscle mitochondrial qualitative properties tend to be more highly conserved. These qualitative properties include enzymatic stoichiometries, respiratory capacity, fuel selection, proton conductance, reactive oxygen species (ROS) production, structural relationship (e.g., cristae surface area-to-volume ratios), and membrane properties (e.g., phospholipid profiles, fluidity). However, even subtle qualitative differences in mitochondrial properties can be important to the tissue. For example, mitochondrial cristae surface area-to-volume ratios are in the range of 20–40 m<sup>2</sup>/ml across vertebrate striated muscles, but can reach as high as 70 m<sup>2</sup>/ml in high-performance species such as hummingbirds (39), antelope (25), and tuna (27).

From one perspective, it is not surprising that many aspects of mitochondrial biogenesis are tightly coordinated to maintain the integrity of such a complex organelle. Recent studies have identified many genetic mechanisms that help coordinate expression of mitochondrial genes (2, 4, 21, 23, 24, 30, 36, 45, 46). However, from another point of view, the process of building mitochondria is so complex that it should not be surprising that differences in mitochondrial enzymatic and functional properties can arise in some situations. Mitochondrial enzyme levels, for example, are most variable during periods of rapid transition, such as exercise training, electrical stimulation, environmental challenges, differentiation, and development. For example, mitochondrial enzymes increase manifold during myogenesis (29) and electrical stimulation of skeletal muscle (13, 14, 34) but individual electron transport system (ETS) and Krebs cycle enzymes do not change in parallel. These transitional situations illustrate that muscles are capable of altering mitochondrial properties, but it is less clear whether muscles in steady state actually maintain qualitatively different mitochondria.

---

The costs of publication of this article were defrayed in part by the payment of page charges. The article must therefore be hereby marked "advertisement" in accordance with 18 U.S.C. Section 1734 solely to indicate this fact.

---

Address for reprint requests and other correspondence: C. D. Moyes, Dept. of Biology, Queen's Univ., Kingston, Ontario, Canada K7L 3N6 (E-mail: moyesc@biology.queensu.ca).

Insight into the origins and significance of mitochondrial specializations can also be gained by comparing the inherent properties of mitochondria from different fiber types within an individual. In general, there have been few studies that have compared muscle mitochondria among striated muscle fibers within individuals (e.g., Refs. 3, 18, 32, 37, 42). This model is useful for assessing the basis of differences in mitochondrial content and the potential for fiber-type specific mitochondrial specializations. Muscle fiber types originate during embryonic development. Although much is known about the regulatory basis of distinct contractile phenotypes (41, 43), myoglobin levels (47), and contractile protein isoform profiles (10), fewer studies have addressed the parallel processes that determine the striated muscle mitochondrial phenotype during differentiation and development (17, 24, 29).

Fiber-type specific fine tuning of mitochondrial properties might be expected in the realm of energetics, ROS production, or proton conductance because of the role of mitochondria in each muscle. For instance, trade-offs between capacity and efficiency might be beneficial. Cardiac muscle mitochondria typically operate close to their maximal capacity (state 3), whereas skeletal muscle mitochondria are most often closer to resting rates (state 4). Mitochondria provide most of the energy for active oxidative muscle fibers, but glycolytic fibers rely upon mitochondria to support basal and recovery metabolism (28). The patterns of recruitment are also relevant to metabolism of ROS. Mitochondrial superoxide production is accelerated at low respiratory rates when electron transport chain complexes are reduced (19). Thus white muscle mitochondria in vivo would be expected to produce more superoxide than those of red or cardiac muscles, based solely on muscle recruitment patterns. Fiber-type differences in ROS production in vivo could impinge on both their cytotoxic and regulatory effects (see Ref. 21). Proton leak across the mitochondrial membrane can influence both the efficiency of energy conversion and the propensity to induce ROS production (see Ref. 38). Although recruitment pattern has a pronounced effect on mitochondrial function, it is not known if different muscle types produce specialized mitochondria to accommodate these differences.

In this study, we examined the nature of fiber type differences in mitochondrial properties in striated muscle of rainbow trout. Fish are useful models with which to explore the determinants of mitochondrial design. Skeletal muscle exists as virtually pure fiber types, with clear delineation of locomotory recruitment patterns. Fiber type differences are also much more extreme in fish. Although white muscle mitochondrial content is similar to mammalian skeletal muscles, the mitochondrial content of fish red muscle is ~10-fold greater, approaching or exceeding that of heart (e.g., Ref. 27). In this study, we compared the structural and functional properties of mitochondria in red, white, and cardiac muscle to determine the extent to which mitochondria exhibit fiber type-specific specializations. We also examined intertissue determinants of mito-

chondrial content across tissues. Collectively our studies identify conserved and malleable mitochondrial properties between fiber types and suggest that even quantitative differences between fiber types may be explained largely by constitutive expression.

## MATERIALS AND METHODS

*Source and maintenance of animals.* Adult male and female rainbow trout (*Oncorhynchus mykiss*) ranging in size from 0.8 to 1.2 kg were purchased from Pure Springs Trout Farm (Belleville, ON, Canada). Fish were held at 15°C in a single flow-through tank under a 12:12-h light/dark photoperiod and fed standard trout chow ad libitum. Fish were killed after anesthetization in MS-222. Tissues were either used directly for mitochondrial isolation or flash frozen in liquid nitrogen. Frozen tissues were powdered under liquid nitrogen and stored at -80°C.

*Mitochondrial isolation and analyses.* Mitochondria from red, white, and cardiac muscle were isolated as previously described (27). Previous studies have found no biochemical differences between subsarcolemmal and interfibrillar mitochondria from trout red muscle (6). In brief, muscle was minced on ice and transferred to 10 vol isolation buffer (in mM: 140 KCl, 5 MgCl<sub>2</sub>, 20 HEPES, 10 EDTA, pH 7.0), supplemented with 0.5% BSA. Samples were homogenized with two passes of a loose-fitting Teflon pestle, followed by three passes with a tight-fitting pestle. Homogenates were then centrifuged at 800 g for 5 min at 4°C, and the supernatant was filtered through eight layers of cheesecloth and recentrifuged. The resultant supernatant was centrifuged at 9,000 g for 10 min. The mitochondrial pellets were resuspended in 12 ml of isolation buffer (-BSA) and recentrifuged and resuspended in the same buffer to a final protein concentration of 4 mg/ml.

Respiration studies were performed as previously described (27). Mitochondria (50 µl) were incubated in 2 ml of respiration medium (in mM: 140 KCl, 20 HEPES, 5 Na<sub>2</sub>HPO<sub>4</sub>, and 0.5% BSA, pH 7.3). Oxygen consumption was monitored polarographically at 15°C using a Clark-type electrode interfaced with Vernier Instruments Data Logger software. Respiratory rates were determined in the presence of succinate (10 mM) or pyruvate (1 mM) with malate (0.1 mM), both in the absence and presence of ADP. State 3 respiration was stimulated by the addition of 0.2 mM ADP. Mitochondria respiring on succinate in state 4 were given rotenone (5.5 µM) and oligomycin (4.5 µg/ml) to determine leak respiration. Respiratory control ratios (RCR), a ratio of the state 3 to state 4 rates, were determined for each mitochondrial preparation (respiring on pyruvate + malate) as an index of mitochondrial quality.

*Proton leak.* Proton leak was measured as described by Brand (8) using respiration conditions outlined above. Membrane potential across the inner mitochondrial membrane was measured concurrently with the rate of mitochondrial respiration, using a triphenylmethylphosphonium (TPMP<sup>+</sup>)-selective electrode constructed from a modified Clark-type oxygen electrode. The TPMP<sup>+</sup> electrode was calibrated after the addition of mitochondria to the reaction vessel by the incremental addition of fixed volumes of TPMP<sup>+</sup> to the mixture up to 5.5 µM. Mitochondrial suspensions (0.3–0.6 mg/ml) were assayed in the presence of rotenone (5.5 µM), TPMP<sup>+</sup> (5.5 µM), succinate (4.5 mM), nigericin (0.55 µg/ml), oligomycin (4.5 µg/ml), ADP (227 µM), and variable amounts of malonate (0–3.75 mM added incrementally). After the malonate titration, 45 nM FCCP was added to the suspension to completely uncouple the mitochondria, thereby dissipating

the membrane potential and releasing the accumulated TPMP<sup>+</sup> from the mitochondrial matrix. This allowed compensation for electrode drift if necessary.

The correction for nonspecific mitochondrial TPMP<sup>+</sup> binding used in calculating the mitochondrial membrane potential was 0.35. This value is the binding correction for rat skeletal muscle as determined by Rolfe et al. (35) and can be used for rainbow trout muscle (red, white, and heart) mitochondria following the justification presented in Brookes et al. (9) for rainbow trout liver mitochondria.

Data acquisition was performed using LabVIEW 4.1 software (National Instruments, Austin, TX) interfaced with National Instruments data-acquisition hardware (National Instruments) and then imported into Logger Pro Version 1.0.2 (Vernier Software, Tufts University) for analysis.

**Membrane fluidity.** Membrane fluidity was measured using methods modified by Williams and Somero (44). Aliquots of frozen mitochondria were thawed on ice and diluted in 2 ml mitochondrial respiration buffer to an absorbance (364 nm) of ~0.15. At the onset of the experiment, 1.5  $\mu$ l of 1,6-diphenyl 1,3,5-hexatriene in 2 mM *N,N'*-dimethylformamide (DPH) was added to samples that were stirred in the dark at room temperature for 30 min. Fluorescence polarization of DPH at various temperatures was measured on a Shimadzu spectrofluorophotometer (RF-5301 PC) equipped with polarization filters and a water-jacketed cell holder. Samples were stirred with a magnetic stirrer throughout the measurement period. Excitation of the DPH was at 364 nm, and fluorescence was detected at 430 nm. Each preparation was measured in duplicate or triplicate at each temperature. Fluorescence polarization, an index of membrane fluidity, was calculated according to Litman and Barenholz (26).

**Enzyme analyses.** Tissue extracts and isolated mitochondria were used to determine enzyme activities per gram tissue and per milligram mitochondrial protein, respectively. Powdered tissue was weighed and solubilized in 9 vol of extraction buffer (20 mM HEPES, pH 7.0, 1 mM EDTA, and 0.1% Triton X-100) using a ground glass tissue homogenizer. Suspensions of isolated mitochondria (4 mg/ml) were diluted with extraction buffer before kinetic measurements. Enzyme activities were determined at 25°C using a Molecular Devices Spectramax 250 spectrophotometer. Assays for citrate synthase (CS; 29), aconitase (11), 2-oxoglutarate dehydrogenase (OGDH; 29),  $\beta$ -hydroxyacyl-CoA dehydrogenase (HOAD; 29), catalase (22), SOD (22) and glutathione peroxidase (GPx; 22) were as previously described. Isolated mitochondria were also used to assess catalytic stoichiometries of complex I, II, II-III, IV, and V (7).

**Mitochondrial H<sub>2</sub>O<sub>2</sub> production.** Mitochondria were incubated in a black 96-well plate (10–20  $\mu$ g per well) in the presence of 90  $\mu$ l of mitochondrial respiration medium, containing 10 mM succinate and H<sub>2</sub>O<sub>2</sub> detection system (Molecular Probes) consisting of 50  $\mu$ M Amplex red and 10 mU horseradish peroxidase (HRP). HRP catalyzes the oxidation of Amplex red by H<sub>2</sub>O<sub>2</sub>, which results in the formation of the fluorescent compound, resorufin (excitation 530, emission 590). The H<sub>2</sub>O<sub>2</sub> standard curve was established with 10  $\mu$ l of freshly prepared H<sub>2</sub>O<sub>2</sub> stock solutions (0.1–5  $\mu$ M) in 90  $\mu$ l respiration medium. BSA (1  $\mu$ l of 10 mg/ml stock) was included in the wells of the H<sub>2</sub>O<sub>2</sub> standard curve to give a final protein content equivalent to the mitochondrial preparations (10  $\mu$ g/well). Fluorescence of the mitochondrial samples and H<sub>2</sub>O<sub>2</sub> standard curve was measured at 0, 15, and 35 min on a Spectramax Gemini fluorometer (Molecular Devices). Between measurements, the samples in the plate were maintained at 15°C in the dark. The production of H<sub>2</sub>O<sub>2</sub> by mitochondria was linear with time over at least 35 min.

**Cytochrome spectra.** Isolated mitochondria (1.5–4 mg/ml) were solubilized for 1 h on ice in 50 mM Tris (pH 8.0) supplemented with 1% Triton X-100. Ultraviolet (UV)-visible spectra were recorded on an OLIS-refurbished Aminco DW-2 UV/VIS spectrophotometer as previously described (22). Spectra are presented as reduced-oxidized differences. The oxidized state is taken as the form of the sample in air and is unchanged on addition of ferricyanide. The reduced state is generated by addition of a few grains of solid sodium dithionite to the air-oxidized sample.

**Electrophoresis and immunoblotting.** Blue native (BN)-PAGE was performed as previously described (22). Isolated mitochondria were solubilized (2 mg/ml) on ice for 30 min in 50  $\mu$ l of 750 mM 6-aminocaproic acid, 50 mM bis-Tris (pH 7.0), 0.5 mM EDTA, and 1% wt/vol lauryl maltoside. Samples were centrifuged for 20 min at 20,000 *g*, loading dye was added to each sample at a 1:4 ratio of Coomassie-lauryl maltoside, and equal amounts of protein were loaded in each lane of a 6–15% continuous gradient gel. Conditions used for electrophoresis, direct immunoblotting, and enhanced chemiluminescence detection of immunoreactive proteins were as previously described (22).

**DNA and RNA isolation and analyses.** Probes for rainbow trout cytochrome oxidase I (COX I) (5) and rat CS (20) were used. The nuclear respiratory factor (NRF)-1 cDNA construct was a generous gift of Dr. R. C. Scarpulla (Northwestern University, Chicago, IL). A cDNA for COX VIa was amplified from a trout red muscle reverse-transcriptase template at 50°C with 5'-AGGACCTGGAAGATCCTG-3' and 5'-TGAGGGTTGTGGAAGAG-3' using standard PCR conditions, cloned into pCR 2.1 (Invitrogen), and sequenced. All radiolabeled probes for Northern blots were prepared by adding 50 ng cDNA and 50  $\mu$ Ci [<sup>32</sup>P]dCTP to Ready-to-Go labeling beads (Pharmacia).

DNA was purified as previously described, using enzyme homogenates as starting material (20). RNA was isolated using acid phenol, as modified for fish muscle (5). Total RNA (5–20  $\mu$ g) was electrophoresed on 1.4% formaldehyde agarose gels and transferred overnight to nylon membrane (Duralon, Stratagene) by capillary transfer in 20 $\times$  SSC. After transfer, the membrane was rinsed with 2 $\times$  SSC, air dried, and UV cross linked.

Membranes were prehybridized, hybridized, and washed as previously described (20). Blots were phosphorimaged and relative signal strength was quantified using Imagequant software (Molecular Dynamics). Differences in loading across lanes were normalized using a probe for 18-S mRNA.

**Statistical analysis.** Proton leak kinetics data were analyzed using Systat 10.2 (Systat Software, Richmond, CA). For all other mitochondrial parameters, significant differences ( $P < 0.05$ ) between fiber types were detected using one-way analysis of variance on ranks and identified using Tukey's test. After statistical analysis, data were scaled relative to heart to facilitate comparisons.

## RESULTS

**Mitochondrial enzyme stoichiometries.** Mitochondria from red, white, and cardiac muscle were isolated to quantify the relative levels of oxidative phosphorylation (OXPHOS) and Krebs cycle enzymes across fiber types (Fig. 1A). The activities of all ETS complexes covaried across tissues. The levels were comparable in red and white muscle, but were ~50% greater in cardiac muscle. Complex V activities were much more similar across tissues. There was also good agreement

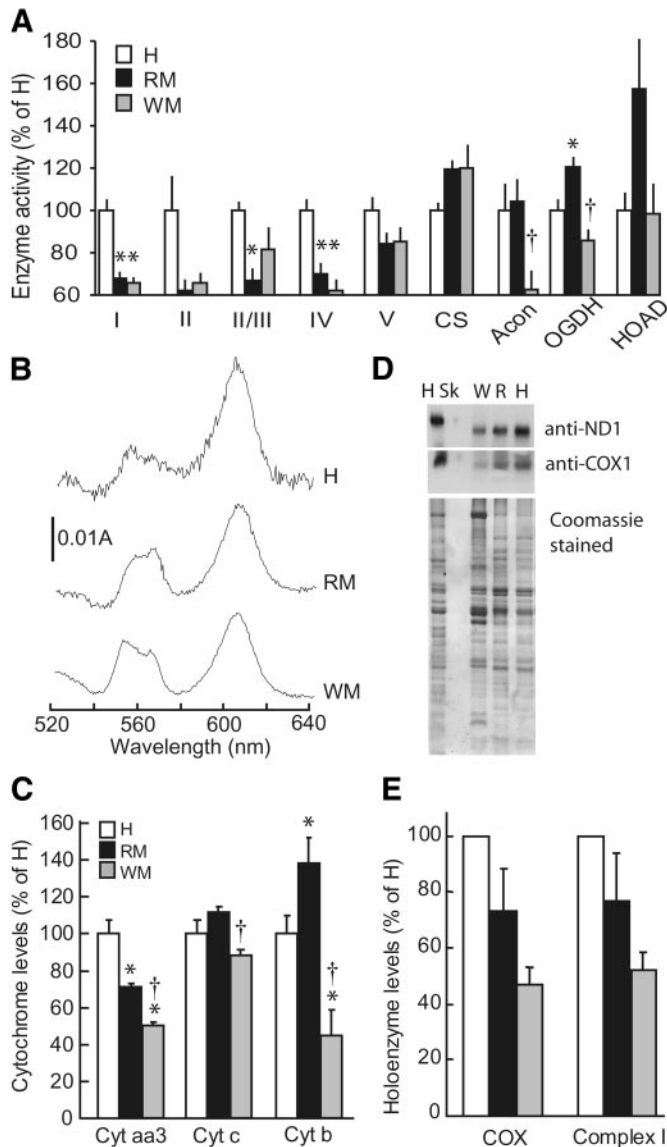


Fig. 1. Biochemical and molecular characterization of oxidative phosphorylation (OXPHOS) complex stoichiometries in mitochondria isolated from red (RM), white (WM), and cardiac (H) muscle. **A**: OXPHOS (complexes I–V), Krebs cycle [2-oxoglutarate dehydrogenase (OGDH), aconitase (Acon), citrate synthase (CS)], and fatty acid oxidation [ $\beta$ -hydroxyacyl-CoA dehydrogenase (HOAD)] enzyme activities across fiber types (means  $\pm$  SE,  $n = 5$ –9). Representative traces (**B**) and content of cytochromes *aa3*, *b*, and *c* obtained from difference spectra (air oxidized-dithionite reduced) of solubilized mitochondria from each fiber type (WM,  $n = 6$ ; RM and H,  $n = 5$ ) (**C**). Immunoblots from first dimension blue native (BN)-PAGE gels of complex I (anti-ND1) and cytochrome oxidase (COX) (anti-COX I) (**D**) and densitometric quantitation of holoenzyme levels across fiber types ( $n = 3$ ) (**E**). For all panels, \*significant difference ( $P < 0.05$ ) from cardiac muscle, and †significant difference between WM and RM. Rates are expressed per mg mitochondrial protein.

between functional and structural indexes of COX. Intertissue patterns in COX (Fig. 1A) were mirrored by cytochrome *aa3* levels (Fig. 1, B and C) and holoenzyme levels, which were determined by immunoblotting of BN-PAGE gels (Fig. 1, D and E). The levels of cytochrome *c* determined spectroscopically were similar across tissues (Fig. 1C). The activity patterns for com-

plex I (Fig. 1A) were also reflected by holoenzyme levels (Fig. 1, D and E). There was less agreement between complex II/III activity and cytochrome *b* levels. It must be kept in mind that the enzymatic assay assesses flux through the complex II/III pair, whereas the spectroscopic assay assesses complex III (cytochrome *b*) levels.

The relationship between Krebs cycle enzymes was somewhat more variable between tissues. Unlike the more strict stoichiometries between ETS complexes, the three Krebs cycle enzymes showed nonstoichiometric relationships (Fig. 1A). Whereas CS activity was similar across tissues, aconitase was 50% lower in white muscle. OGDH in red muscle was 20% higher than heart, and white muscle was 20% lower than heart. The activity of HOAD, an enzyme involved in fatty acid oxidation, was similar in heart and white muscle but 60% higher in red muscle.

**Mitochondrial respiration rates and leak kinetics.** Rates of mitochondrial respiration were measured to address the impact of enzymatic patterns on functional properties of mitochondria across striated muscle fibers (Fig. 2A). State 3 respiration rates in cardiac muscle mitochondria were twofold higher than either red or white muscle. The intertissue pattern in respiration is identical to that for COX, the terminal step of the ETS (Fig. 1A).

The respiratory properties (pyruvate plus malate) were very similar in mitochondria from each muscle type. The state 2 rate (before ADP addition) was 5–7% of the maximal state 3 rates in all tissues (Fig. 2A). State 4 rates (after ADP phosphorylation) were higher and more variable than state 2 rates, which we attribute to variable amounts of contaminating ATPases arising in the different fiber types.

The leak properties of mitochondria were also similar in all mitochondria. Leak respiration (i.e., succinate-based respiration in the presence of rotenone and oligomycin) was ~9–12% of the maximal state 3 respiratory rates in mitochondria from all tissues (Fig. 2A). Leak kinetics were assessed using malonate titrations in conjunction with TPMP<sup>+</sup> (Fig. 2B). In Fig. 2B, membrane potential is plotted against respiration rate, expressed per milligram protein. The overlap in the curves suggests that the three preparations exhibit the same proton conductance. The proton conductances can be estimated from the membrane potential, respiration rate, and  $H^+/O_2$  for mitochondria, as described by Nicholls and Ferguson (31) (Table 1). For example, at 150 mV, each preparation has a similar proton conductance of ~0.27 nmol  $H^+$ /min/mV/mg protein (Table 1). Although proton conductances are usually estimated expressed relative to milligram mitochondrial protein, they should ideally be expressed per unit surface area of inner mitochondria, the barrier in the circuit. Studies that express conductance relative to milligram mitochondrial protein use an implicit assumption that it correlates with inner membrane surface area. We believe that in these mitochondria, COX is a more realistic index of mitochondrial inner membrane surface area. When we assess proton leak kinet-

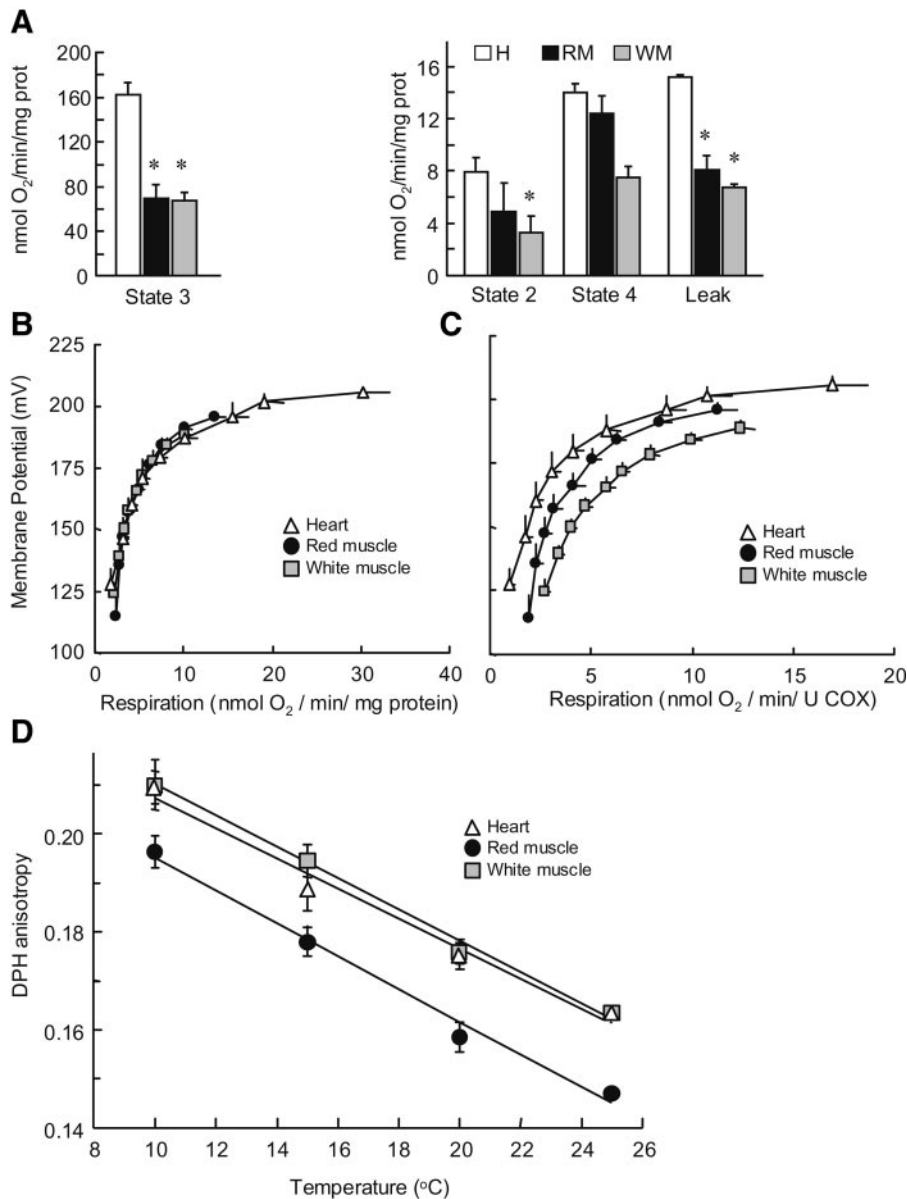


Fig. 2. Biochemical characterization of mitochondrial respiration, leak kinetics, and membrane fluidity in mitochondria isolated from RM, WM, and H muscle. *A*: respiration rates (1 mM pyruvate plus 0.1 mM malate) across fiber types (WM,  $n = 7$ ; RM,  $n = 6$ ; H,  $n = 5$ ). *B*: mitochondrial membrane potential is plotted as a function of respiration rate, expressed per mg mitochondrial protein (WM,  $n = 7$ ; RM,  $n = 6$ ; H,  $n = 5$ ). *C*: values shown in *B* were replotted using U COX activity as the denominator. COX specific activities are shown in Table 1. *D*: anisotropy plots of 1,6-diphenyl 1,3,5-hexatriene in 2 mM in *N,N'*-dimethylformamide (DPH) fluorescence depicted as a function of temperature ( $n = 5$ ). Mitochondrial membrane fluidity is inversely related to anisotropy. For *A*, \*significant difference ( $P < 0.05$ ) from H muscle.

ics using the alternative denominator of COX activity, apparent differences in proton conductance emerge (Fig. 2C). At 150 mV, the proton conductance of white muscle mitochondria is more than twice that of heart and red is intermediate. This pattern is similar across the entire ohmic range of the curve. These analyses lead us to conclude that there are real differences in proton conductance in mitochondria of red, white, and cardiac muscles.

**Membrane fluidity.** The local lipid environment can affect the structure and function of mitochondrial proteins. As a result, potential differences across fiber types in mitochondrial membrane fluidity were quantified using DPH anisotropy (Fig. 2D). The temperature dependence of membrane fluidity (i.e., slope of anisotropy vs. temperature) was similar across fiber types (Fig. 2D). However, the membrane fluidity of red muscle was significantly greater than either cardiac or

Table 1. Proton conductance in isolated mitochondria respiring on succinate

Tissue	Membrane Potential, mV	Respiration, nmol O <sub>2</sub> /min/mg protein	Proton Conductance, nmol H <sup>+</sup> /min/mV/mg protein	
			nmol H <sup>+</sup> /min/mV/U COX	
<i>High membrane potential</i>				
Heart	185	9.32	0.60	0.34
Red muscle	185	7.87	0.51	0.42
White muscle	185	8.58	0.56	0.68
<i>Low membrane potential</i>				
Heart	150	3.40	0.27	0.15
Red muscle	150	3.46	0.28	0.23
White muscle	150	3.29	0.26	0.32

Proton conductance assumes an H<sup>+</sup>/O of 6. Cytochrome oxidase (COX) activities were 1.78, 1.21, and 0.82 U/mg protein in heart, red and white muscle, respectively.

white muscle; the fluidity of red muscle mitochondrial membranes at 15°C was equivalent to that of cardiac muscle and white muscle at 20°C.

**Mitochondrial ROS production.** ROS release by mitochondria into the extramitochondrial space is likely influenced by many factors affecting its synthesis and degradation. Functional parameters that could influence ROS production include differences in enzyme stoichiometries, respiratory rates, and leak kinetics. When we assessed H<sub>2</sub>O<sub>2</sub> release, we found the inter-tissue pattern resembled that of OXPHOS proteins, such as COX (Figs. 1A and 3A). The activities of both mitochondrial MnSOD and GPx also paralleled COX activities (Figs. 1A and 3B). Collectively, these data suggest little evidence for interfiber differences in mitochondrial ROS production or protection.

We also assessed the relationship between fiber type mitochondrial content and antioxidant enzymes. In general the whole tissue activities of catalase, GPx, and total cellular SOD were strongly correlated with COX activities (Fig. 3, C–E).

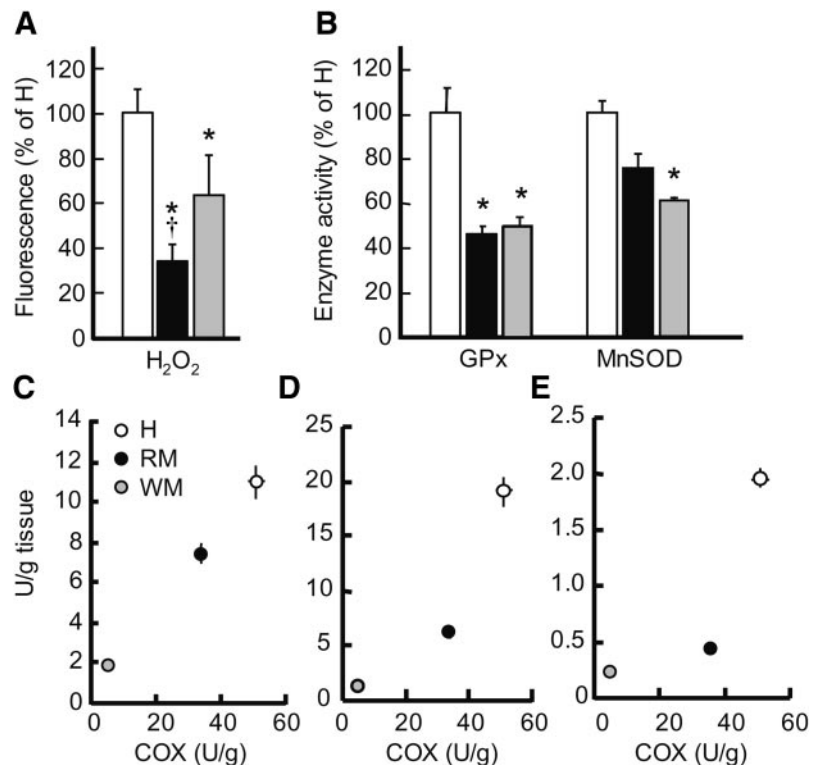
**Differences in COX gene expression across fiber types.** We assessed the relative levels of COX gene transcripts in relation to COX enzyme content and COX gene content (Fig. 4). For both mtDNA-encoded COX I and nuclear-encoded COX VIa, the levels of transcripts paralleled COX content when expressed per gram tissue (Fig. 4C). Similar differences across fiber types were also observed for two additional nuclear-encoded transcripts, CS and NRF-1 (Fig. 4, B and C). We sought to express these patterns relative to gene levels to take into account differences in fiber morphology. Total DNA levels in heart were approximately twofold

greater than red muscle and sixfold greater than white muscle (Fig. 4C). When transcript levels were expressed relative to DNA content, most of the differences between fiber types were greatly diminished (Fig. 4D). Similarly, when COX activity (which is representative of the activity of other OXPHOS complexes) in individual fiber types was expressed relative to DNA, only minor differences were observed. Collectively, these data suggest that constitutive pathways that transcend fiber types are primarily responsible for determining quantitative and qualitative properties of mitochondria.

## DISCUSSION

Discussion of the relationship between muscle activity and bioenergetic gene expression is fraught with contradictions. Because mitochondria are required in most tissues to maintain energy homeostasis, mitochondrial enzymes are often considered to be house-keeping genes under the control of constitutive pathways. Yet different muscle fibers possess a broad range of mitochondrial contents. Although the developmental determinants of the contractile phenotypes in different muscle types are well understood, the origins of the bioenergetic phenotypes are not. In addition to developmental plasticity in mitochondrial enzyme content, mature muscles show considerable capacity to alter mitochondrial content in relation to activity levels. Although there is considerable variation in the mitochondrial quantities between fiber types, it is not yet clear if the mitochondria have distinct compositions and/or functional properties. In this study we have

Fig. 3. Mitochondrial antioxidant enzyme content and rates of succinate-dependent H<sub>2</sub>O<sub>2</sub> production. **A:** Amplex red fluorescence measurements of the rate of succinate-dependent mitochondrial H<sub>2</sub>O<sub>2</sub> production under state 4 respiration conditions (H, *n* = 6; WM and RM, *n* = 7). Values were determined per mg protein, then scaled to be expressed relative to heart mitochondria. **B:** mitochondrial antioxidant enzyme activity [Mn superoxide dismutase (SOD), glutathione peroxidase (GPx)] (*n* = 5–9). **A and B:** \*significant difference (*P* < 0.05) from cardiac muscle, and †significant difference between RM and WM. Values were determined per mg protein, then scaled to be expressed relative to heart mitochondria. **C–E:** relationship between the activities of COX and the antioxidant enzymes SOD (C), catalase (D), and GPx (E) (*n* = 5, all tissues).



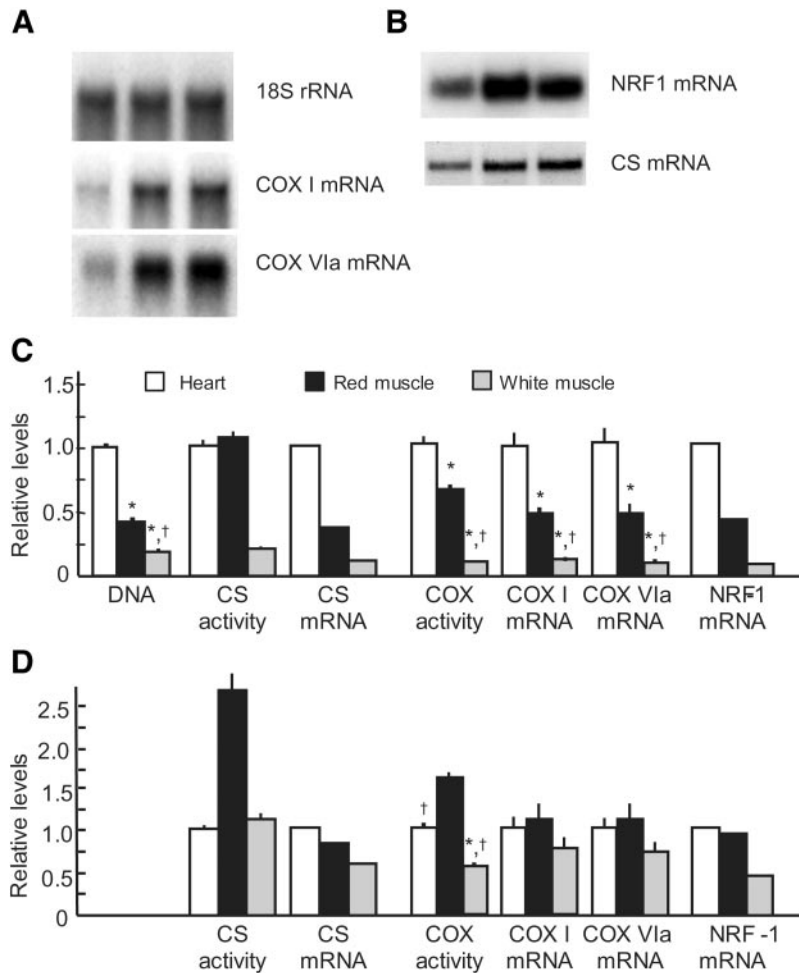


Fig. 4. Quantitative and qualitative differences in mitochondrial properties are not reflected in substantial differences in gene expression. *A*: representative Northern blots of 10  $\mu$ g total RNA probed for COX I and COX VIa and normalized for loading with 18S ( $n = 5$ ). *B*: Northern blot with 2  $\mu$ g poly A<sup>+</sup> blot probed for nuclear respiratory factor (NRF)-1 and CS ( $n = 1$ ). Poly A<sup>+</sup> blot was also probed with COX VIa, which served as an internal loading control. *C*: relative levels of DNA, CS, and COX activities and RNA expressed per g tissue. *D*: data in *C* transformed to compare levels relative to genomic DNA. For *C* and *D*, significant difference ( $*P < 0.05$ ) from H muscle and  $\dagger$  significant difference between RM and WM.

attempted to reconcile constraints on mitochondrial design, with distinct functional responsibilities and the potential role of mitochondria in mediating retrograde signaling.

Comparison of mitochondrial properties between tissues demands careful attention to the choice of denominator. Most studies use milligram mitochondrial protein as a denominator for mitochondrial enzymes and processes. In any pure mitochondrial preparation, most of the protein probably exists within the inner membrane and consists primarily of the proteins of the electron transport chain and the adenine nucleotide translocase. Consequently, milligram protein is usually a good indicator of a unit of mitochondria because of its tendency to correlate with important structural (e.g., cristae surface area) and functional (respiratory rate, proton conductance) parameters. It is important, however, to recognize that using milligram protein as a denominator to express mitochondrial parameters involves an implicit assumption that may not always be valid. For example, exercise in rats causes a 55–60% increase in mitochondrial protein, whereas COX and other ETS enzymes increase twofold (see Ref. 16). Thus, in this study, COX (or any other index of ETS activity) appears to be a more relevant indicator of the metabolic potential of mitochondria.

*Are mitochondria similar across fiber type?* The conclusions on the extent of fiber type differences are entirely dependent on which denominator is chosen. We found (Fig. 2A), as have others (e.g., tuna, Ref. 27; rats, Ref. 12), that the maximal respiratory rate (per mg protein) of heart mitochondria is greater than that of skeletal muscle mitochondria. However, we also found that heart mitochondria have elevated specific activities of COX, as well as other ETS complexes. Thus, if we compare the patterns of respiratory rates with the relationships in COX and OXPHOS complexes, the apparent differences between fiber types largely disappear. For the most part, our enzymatic analyses, spectroscopic measurements of cytochrome content, and immunoblotting of BN-PAGE gels indicate a strong relationship between these complexes in each tissue.

Not all of the mitochondrial parameters we studied were similar across tissues. In contrast to the strict stoichiometries seen with OXPHOS activities, the relationship between other mitochondrial enzymes was more variable. Although much is known about the control of expression of OXPHOS genes, very little is known about the transcriptional control of Krebs cycle enzymes. The relationships between Krebs cycle enzymes are not always rigidly preserved in muscles. For

example, mitochondria from rat soleus (I) and gracilis (IIb) have slightly different stoichiometries in malate dehydrogenase and CS (18). Exercise in rats causes a twofold increase in CS and isocitrate dehydrogenase, but OGDH and mitochondrial malate dehydrogenase increase only ~50% (16). The activity of the fatty acid oxidizing enzyme HOAD also appeared elevated in red muscle skeletal muscle mitochondria (Fig. 1A). Metabolically, mitochondria from oxidative fiber types often exhibit enzymatic or metabolic properties that suggest a predisposition toward fatty acids as fuel (e.g., rabbit, Refs. 3, 18; fish, Refs. 29, 27), which is in contrast to what is observed in response to exercise training or electrical stimulation (16). There also appeared to be fiber-type differences in mitochondrial membrane fluidity (Fig. 2D). Differences in fluidity of mitochondrial membranes can be due to many factors including phospholipid profiles (chain length, saturation, cardiolipin content). Such differences could affect the in vivo activity of many membrane bound enzymes, including ETS complexes (15). Although our assays did not reveal differences in maximal activities of OXPHOS complexes, it is possible that fluidity and/or membrane properties could influence other aspects of ETS kinetics.

The general similarity in mitochondrial design also extended to other structural and functional features. Movement of protons across the mitochondrial inner membrane dissipates  $\Delta\Psi$  and allows electron transport activity. Protons can cross the inner membrane through the phospholipid bilayer, a process that may be facilitated either through nonspecific integral membrane proteins or through specific leak pathways such as uncoupling proteins (38). When we compared proton leak kinetics in fiber types, our conclusions depended on the denominator chosen to equalize preparations. By the traditional calculation (based on mg mitochondrial protein), there would appear to be no difference in proton conductance based on the overlap in the curves (Fig. 2B) and calculated proton conductances at high and low membrane potential (Table 1). We have argued that COX is probably a better indicator of inner membrane surface area and, consequently, a better denominator against which to assess proton conductance (Fig. 2C). This leads us to conclude that proton conductance decreased in the following order: white muscle > red muscle > heart (Table 1). Although the exact nature of the proton leak is not clear, it is intriguing that proton conductance did not appear to parallel the activities of the ETS, and presumably inner membrane surface area. The distribution and content of uncoupling protein isoforms have not been assessed in fish muscle.

Mitochondrial ROS production depends on the factors that influence superoxide production and the nature of the antioxidant defenses. Mitochondrial ROS production arises when molecular oxygen steals electrons from complex I and III to produce superoxide, which is rapidly scavenged by mitochondrial MnSOD, releasing  $H_2O_2$  into the cytosol. As mentioned, normal mitochondrial ROS production is significant only when respiration is inhibited by high membrane potential,

which would accompany state 4 conditions (19) or during hypoxia (33). As with proton conductance, the interpretation of fiber-type differences in mitochondrial ROS production is influenced by the denominator. When expressed relative to milligram mitochondrial protein, heart mitochondria appear to produce two to three times more  $H_2O_2$  than do the skeletal muscles (Fig. 3A). Again, this difference largely disappears when ROS production is expressed relative to COX activity. Similarly, MnSOD and GPx are generally higher in heart than either red and white muscle enzymes, but these differences are reduced when expressed relative to COX. Despite the similarity of the rates of  $H_2O_2$  production and ROS scavenging by isolated mitochondria in vitro, it is likely that recruitment pattern would influence ROS kinetics in vivo. Because white muscle mitochondria are typically near state 4 in vivo (28), ROS production is likely highest in this tissue. In contrast, heart mitochondria in vivo would rarely approach state 4 and therefore would be expected to produce little ROS under most conditions. Because the antioxidant enzyme activities in mitochondria correlate with respiration capacity and ETS enzymes, there is little indication of fiber-type specific mitochondrial fine tuning in the context of ROS defense.

*Origins of variation in mitochondrial content.* Control of mitochondrial quantitative and qualitative properties during mitochondrial biogenesis may be governed by both constitutive and inducible/adaptive pathways. Recent studies have provided insight into the role of gene regulation in mediating variation in mitochondrial content between physiological states (see Refs. 30, 36). Mitochondrial genes typically lack TATA boxes but possess CAAT boxes and GC boxes that may govern constitutive gene expression. Coordination of adaptive changes in mitochondrial genes may be mediated by overlapping sensitivities to inducible transcriptional activators such as nuclear respiratory factor-1 (NRF-1) and NRF-2 (for OXPHOS genes) and peroxisome proliferator-activated receptors (PPAR; for fatty acid  $\beta$ -oxidation genes; 4, 36). Also, the PPAR- $\gamma$  coactivator-1 (PGC-1) family (PGC-1 $\alpha$ , PGC1-related coactivator and PGC-1 $\beta$ ) helps to coordinate expression of nuclear-encoded mitochondrial genes (2, 24, 36). Transgenic mouse studies have implicated several proteins as determinants of mitochondrial content, including myogenin (17), PGC-1 (23, 45), and its regulators, such as calmodulin-dependent protein kinase (46). Changes in PGC-1 activity may be the primary mediator of adaptive changes in mitochondrial properties with exercise training (2). These studies identify potential regulators of mitochondrial content within individual muscles, perhaps suggesting the regulatory basis of mitochondrial differences between muscle fiber types.

Our data suggest that many enzymatic features of mitochondrial design are preserved across muscle fiber types. This maintenance of mitochondrial qualitative properties (e.g., enzyme stoichiometries) is consistent with fixed patterns of constitutive expression of respiratory genes. But can a constitutive pattern of gene

expression be reconciled with the well-established quantitative differences in mitochondrial content between fiber types? Do tissues with greater mitochondrial content (per g tissue) necessarily require greater rates of respiratory gene expression? In assessing the origins of mitochondrial differences between fiber types, the differences in nuclear content of muscle fibers must be considered. The myonuclear domain in muscle (the volume of cytoplasm controlled by an individual muscle nucleus) is somewhat plastic during development and adaptation (1). Mature red muscle myonuclei appear to have smaller domains, i.e., higher nuclear content per volume tissue (42). If myonuclei in red and white muscle demonstrated equal levels of transcriptional activity, some differences in mitochondrial biogenesis could accrue due simply to differences in nuclear content and fiber morphometry.

We compared the enzyme activities, mRNA and DNA for COX subunits, to better understand the basis of intertissue differences in mitochondrial enzyme content. The mass-specific activities of the mitochondrial enzymes CS and COX are 5- to 10-fold greater in heart and red muscle relative to white muscle (Fig. 4C). This range is similar to that found in comparing fiber types across other vertebrates. RNA levels for the enzymes (also expressed per g tissue) for the most part parallel enzyme levels. A similar relationship is seen with NRF-1 mRNA, a potential regulator of mitochondrial genes. These patterns are consistent with transcriptional regulation of mitochondrial enzyme levels.

When these parameters are expressed relative to DNA content (Fig. 4D), rather than tissue mass (Fig. 4C), much of the intertissue variation in levels is lost. In other words, the transcript levels for the COX subunits depend largely on the nuclear content of the fiber. White muscle has larger muscle fibers with a lower nuclear content per gram. However, CS genes within white muscle generate the same level of CS transcripts as the CS genes within heart. Superimposed on these simple relationships are suites of posttranscriptional and posttranslation processes. But it appears as if there is no need to invoke differential mitochondrial gene regulation to explain differences in muscle mitochondrial content in striated muscles. Collectively, these studies suggest constitutive pathways that transcend fiber types are primarily responsible for determining both quantitative and qualitative properties of mitochondria.

We thank G. Somero for assistance with spectrofluorometric analysis of membrane fluidity.

Present address for S. C. Leary: Department of Molecular Neurogenetics Rm 676, Montreal Neurological Institute, Montreal, Quebec, Canada H3A 2B4.

## DISCLOSURES

These studies were supported by National Sciences and Engineering Research Council through Discovery Grants (to C. D. Moyes and J. S. Ballantyne) and a postgraduate scholarship (to S. C. Leary), and through personnel support from the Ontario Ministry of Science and Technology through a Premier's Research Excellence Award (to C. D. Moyes).

## REFERENCES

- Allen DL, Roy RR, and Edgerton VR. Myonuclear domains in muscle adaptation and disease. *Muscle Nerve* 22: 1350–1360, 1999.
- Baar K, Wende AR, Jones TE, Marison M, Nolte LA, Chen M, Kelly DP, and Holloszy JO. Adaptations of skeletal muscle to exercise: rapid increase in the transcriptional coactivator PGC-1. *FASEB J* 16: 1879–1886, 2002.
- Baldwin KM, Klinkerfuss GH, Terjung RL, Mole PA, and Holloszy JO. Respiratory capacity of white, red and intermediate muscle: adaptive response to exercise. *Am J Physiol* 222: 373–378, 1972.
- Barger PM and Kelly DP. PPAR signaling in the control of cardiac energy metabolism. *Trends Cardiovasc Med* 10: 238–245, 2000.
- Battersby BJ and Moyes CD. Influence of acclimation temperature on mitochondrial DNA, RNA, and enzymes in skeletal muscle. *Am J Physiol Regul Integr Comp Physiol* 275: R905–R912, 1998.
- Battersby BJ and Moyes CD. Are there distinct subcellular populations of mitochondria in rainbow trout red muscle? *J Exp Biol* 201: 2455–2460, 1998.
- Bindoff LA, Desnuelle C, Birch-Machin MA, Pellissier JF, Serratrice G, Dravet C, Bureau M, Howell N, and Turnbull DM. Multiple defects of the mitochondrial respiratory chain in a mitochondrial encephalopathy (MERRF): a clinical, biochemical and molecular study. *J Neurol Sci* 102: 17–24, 1991.
- Brand MD. Measurement of mitochondrial protonmotive force. In: *Bioenergetics, A Practical Approach*, edited by Brown GC and Cooper CE. New York: IRL, 1995, p. 39–62.
- Brookes PS, Buckingham JA, Tenreiro AM, Hulbert AJ, and Brand MD. The proton permeability of the inner membrane of liver mitochondria from ectothermic and endothermic vertebrates and from obese rats: correlations with standard metabolic rate and phospholipid fatty acid composition. *Comp Biochem Physiol* 119B: 325–334, 1996.
- Calvo S, Vullhorst D, Venepally P, Cheng J, Karavanova I, and Buonanno A. Molecular dissection of DNA sequences and factors involved in slow muscle-specific transcription. *Mol Cell Biol* 21: 8490–8503, 2001.
- Das N, Levine RL, Orr WC, and Sohal RS. Selectivity of protein oxidative damage during aging in *Drosophila melanogaster*. *Biochem J* 360: 209–216, 2001.
- Dohm GL, Huston RL, Askew EW, and Weiser PC. Effects of exercise on activity of heat and muscle mitochondria. *Am J Physiol* 223: 783–787, 1972.
- Hendriksson J, Chi MMY, Hintz CS, Young DA, Kaiser KK, Salmons S, and Lowry OH. Chronic stimulation of mammalian muscle: changes in enzymes of six metabolic pathways. *Am J Physiol Cell Physiol* 251: C614–C632, 1986.
- Hendriksson J, Salmons S, and Lowry OH. Chronic stimulation of mammalian muscle: enzyme and metabolic changes in individual fibers. *Biomed Biochim Acta* 5/6: S445–S454, 1989.
- Hochachka PW and Somero GN. *Biochemical Adaptations*. Princeton, NJ: Princeton University Press, 2002.
- Holloszy JO. Adaptation of skeletal muscle to endurance exercise. *Med Sci Sports* 7: 155–164, 1975.
- Hughes SM, Chi MM, Lowry OH, and Gundersen K. Myogenin induces a shift of enzyme activity from glycolytic to oxidative metabolism in muscles of transgenic mice. *J Cell Biol* 145: 633–642, 1999.
- Jackman MR and Willis WT. Characteristics of mitochondria isolated from type I and type IIb skeletal muscle. *Am J Physiol Cell Physiol* 270: C673–C678, 1996.
- Korshunov SS, Skulachev VP, and Starkov AA. High protonic potential actuates a mechanism of production of reactive oxygen species in mitochondria. *FEBS Lett* 416: 15–18, 1997.
- Leary SC, Battersby BJ, and Moyes CD. Inter-tissue differences in mitochondrial enzyme activity, RNA and DNA in rainbow trout (*Oncorhynchus mykiss*). *J Exp Biol* 201: 3377–3384, 1998.
- Leary SC and Moyes CD. The effects of bioenergetic stress and redox balance on the expression of genes critical to mitochondrial

- function. In: *Cell and Molecular Responses to Stress*, edited by Storey KB and Storey J. New York: Elsevier, 2000, p. 209–229.
22. **Leary SC, Hill BC, Lyons CN, Carlson CG, Michaud D, Kraft C, Ko K, Glerum DM, and Moyes CD.** Chronic treatment with azide in situ leads to an irreversible loss of cytochrome c oxidase activity via holoenzyme dissociation. *J Biol Chem* 277: 11321–11328, 2002.
  23. **Lehman JJ, Barger PM, Kovacs A, Saffitz JE, Medeiros DM, and Kelly DP.** Peroxisome proliferator-activated receptor gamma coactivator-1 promotes cardiac mitochondrial biogenesis. *J Clin Invest* 106: 847–856, 2000.
  24. **Lin J, Wu H, Tarr PT, Zhang CY, Wu Z, Boss O, Michael LF, Puigserver P, Isotani E, Olson EN, Lowell BB, Bassel-Duby R, and Spiegelman BM.** Transcriptional co-activator PGC-1 alpha drives the formation of slow-twitch muscle fibres. *Nature* 418: 797–801, 2002.
  25. **Lindstedt SL, Hokanson JF, Wells DJ, Swain SD, Hoppeler H, and Navarro V.** Running energetics in the pronghorn antelope. *Nature* 353: 748–750, 1991.
  26. **Litman BJ and Barenholz Y.** Fluorescent probe: diphenylhexatriene. *Methods Enzymol* 81: 678–685, 1982.
  27. **Moyes CD, Mathieu-Costello OA, Brill RW, and Hochachka PW.** Mitochondrial metabolism of cardiac and skeletal muscle from a fast (*Katsuwonis pelamis*) and a slow (*Cyprinus carpio*) fish. *Can J Zool* 70: 1246–1253, 1992.
  28. **Moyes CD, Schulte PM, and Hochachka PW.** Recovery metabolism in fish white muscle: the role of the mitochondria. *Am J Physiol Regul Integr Comp Physiol* 262: R295–R304, 1992.
  29. **Moyes CD, Mathieu-Costello OA, Tsuchiya N, Filburn C, and Hansford RG.** Mitochondrial biogenesis during cellular differentiation. *Am J Physiol Cell Physiol* 272: C1345–C1351, 1997.
  30. **Moyes CD and Hood DA.** Origins and consequences of mitochondrial variation in vertebrate muscle. *Ann Rev Physiol* 65: 177–201, 2003.
  31. **Nicholls DG and Ferguson SJ.** *Bioenergetics 2*. San Diego: Academic, 1992.
  32. **Pande SV and Blanchaer MC.** Carbohydrate and fat in energy metabolism of red and white muscle. *J Biol Chem* 220: 549–553, 1971.
  33. **Pearlstein DP, Ali MH, Mungai PT, Hynes KL, Gewertz BL, and Schumacker PT.** Role of mitochondrial oxidant generation in endothelial cell responses to hypoxia. *Arterioscler Thromb Vasc Biol* 22: 566–573, 2002.
  34. **Reichmann H, Wasl R, Simoneau JA, and Pette D.** Enzyme activities of fatty acid oxidation and the respiratory chain in chronically stimulate fast-twitch muscle of the rabbit. *Pflügers Arch* 418: 572–574, 1991.
  35. **Rolfe DFS, Hulbert AJ, and Brand MD.** Characteristics of mitochondrial proton leak and control of oxidative phosphorylation in the major oxygen-consuming tissues of the rat. *Biochim Biophys Acta* 1118: 405–416, 1994.
  36. **Scarpulla RC.** Nuclear activators and coactivators in mammalian mitochondrial biogenesis. *Biochim Biophys Acta* 1576: 1–14, 2002.
  37. **Schwerzmann K, Hoppeler H, Kayar SR, and Weibel ER.** Oxidative capacity of muscle and mitochondria: correlation of physiological, biochemical, and morphometric characteristics. *Proc Natl Acad Sci USA* 86: 1583–1587, 1989.
  38. **Stuart JA, Cadenas S, Jekabsons MB, Roussel D, and Brand MD.** Mitochondrial proton leak and the uncoupling protein 1 homologues. *Biochim Biophys Acta* 1504: 144–158, 2001.
  39. **Suarez RK, Lighton JR, Brown GS, and Mathieu-Costello O.** Mitochondrial respiration in hummingbird flight muscles. *Proc Natl Acad Sci USA* 88: 4870–4873, 1991.
  40. **Suarez RK.** Upper limits to mass-specific metabolic rates. *Annu Rev Physiol* 58: 583–605, 1996.
  41. **Te KG and Reggiani C.** Skeletal muscle fiber type specification during embryonic development. *J Muscle Res Cell Motil* 23: 65–69, 2002.
  42. **Tseng BS, Kasper CE, and Edgerton VR.** Cytoplasm-to-myonucleus ratio and succinate dehydrogenase activities in adult rat slow and fast muscle fibers. *Cell Tissue Res* 275: 39–49, 1994.
  43. **Wigmore PM and Evans DJ.** Molecular and cellular mechanisms involved in the generation of fiber diversity during myogenesis. *Int Rev Cytol* 216: 175–232, 2002.
  44. **Williams E and Somero GN.** Seasonal-, tidal-cycle- and microhabitat-related variation in membrane order of phospholipid vesicles from gills of the intertidal mussel *Mytilus californianus*. *J Exp Biol* 199: 1587–1596, 1996.
  45. **Wu Z, Puigserver P, Andersson U, Zhang C, Adelmant G, Mootha V, Troy A, Cinti S, Lowell B, Scarpulla RC, and Spiegelman BM.** Mechanisms controlling mitochondrial biogenesis and respiration through the thermogenic coactivator PGC-1. *Cell* 98: 115–24, 1999.
  46. **Wu H, Kanatous SB, Thurmond FA, Gallardo T, Isotani E, Bassel-Duby R, and Williams RS.** Regulation of mitochondrial biogenesis in skeletal muscle by CaMK. *Science* 296: 349–352, 2002.
  47. **Yan Z, Serrano AL, Schiaffino S, Bassel-Duby R, and Williams RS.** Regulatory elements governing transcription in specialized myofiber subtypes. *J Biol Chem* 276: 17361–17366, 2001.